

Line and boundary tensions on approach to the wetting transition

K. Koga^{a)} and B. Widom

*Department of Chemistry, Faculty of Science, Okayama University, Okayama 700-8530, Japan and
Department of Chemistry, Baker Laboratory, Cornell University, Ithaca, New York, 14853-1301, USA*

(Received 5 April 2007; accepted 1 June 2007; published online 13 August 2007)

A mean-field density-functional model often used in the past in the study of line and boundary tensions at wetting and prewetting transitions is reanalyzed by extensive numerical calculations, approaching the wetting transition much more closely than had previously been possible. The results are what are now believed to be definitive for the model. They include strong numerical evidence for the presence of the logarithmic factors predicted by theory both in the mode of approach of the prewetting line to the triple-point line at the point of the first-order wetting transition and in the line tension itself on approach to that point. It is also demonstrated with convincing numerical precision that the boundary tension on the prewetting line and the line tension on the triple-point line have a common limiting value at the wetting transition, again as predicted by theory. As a by product of the calculations, in the model's symmetric three-phase state, far from wetting, it is found that certain properties of the model's line tension and densities are almost surely given by simple numbers arising from the symmetries, but proving that these are exact for the model remains a challenge to analytical theory. © 2007 American Institute of Physics. [DOI: 10.1063/1.2752156]

I. INTRODUCTION

Three fluid phases α , β , and γ may meet either in a line of common contact or with one of them spread at the interface between the other two. In the latter case the intruding phase, say β , is said to wet the $\alpha\gamma$ interface. The transition between those two modes of contact of the three phases is the wetting transition.¹⁻⁴ It may be viewed as a transition in the structure of the $\alpha\gamma$ interface, between one in which that interface does not, and one in which it does, consist of a layer of a macroscopic β phase.

The condition that the phases meet in a line of common contact is that the three interfacial tensions $\sigma_{\alpha\beta}$, $\sigma_{\beta\gamma}$, $\sigma_{\alpha\gamma}$ satisfy among themselves the triangle inequalities (Neumann triangle⁵), so that in particular the largest, say $\sigma_{\alpha\gamma}$, be less than the sum of the two smaller: $\sigma_{\alpha\gamma} < \sigma_{\alpha\beta} + \sigma_{\beta\gamma}$. By contrast, the condition that β wet the $\alpha\gamma$ interface is the equality (Antonoff's rule^{5,6}) $\sigma_{\alpha\gamma} = \sigma_{\alpha\beta} + \sigma_{\beta\gamma}$.

Associated with a line of common contact, when $\sigma_{\alpha\gamma} < \sigma_{\alpha\beta} + \sigma_{\beta\gamma}$, is an excess free energy per unit length of the line, which is the line tension, τ .^{5,7-19} A different linear tension, the boundary tension, τ_b , is the tension of the boundary line that separates two coexisting surface phases.^{11,14,20,21} It is thus analogous to a surface tension, σ , but in two rather than three dimensions. While a line tension τ may be of either sign,^{5,7} a boundary tension τ_b , like a surface tension σ , is necessarily positive.

Often associated with a first-order wetting transition in three-phase equilibrium is a prewetting transition, in which phase β , say, is not present as a bulk phase but comes to be anticipated by the sudden appearance of a β -like layer in the $\alpha\gamma$ interface. This is illustrated in Fig. 1, which is for the case of a two-component mixture, showing its line of triple

points and prewetting line as projected onto the plane of two of the mixture's three thermodynamic field variables, called μ_1 and μ_2 in the figure. The α, β, γ triple-point line is AB; the wetting transition occurs at W. The prewetting line is CW. In the three-dimensional thermodynamic space the prewetting line lies in the $\alpha\gamma$ coexistence surface, where it is tangent to the triple-point line at W.²²

In states on the triple-point line below W the β phase does not wet the $\alpha\gamma$ interface; in states above W, it does. In states on the $\alpha\gamma$ coexistence surface far from the triple-point line the $\alpha\gamma$ interface is thin, with a structure unlike that of the bulk β phase; but as the point representing the state of two-phase $\alpha\gamma$ coexistence crosses the prewetting line, there is a discontinuous change in the structure of the $\alpha\gamma$ interface, to one that is thick and reminiscent of bulk β . As the representative point on the $\alpha\gamma$ coexistence surface approaches the triple-point line, in the region between CW and WB in the figure, the β -like layer thickens, until the triple-point line itself is reached, when the $\alpha\gamma$ interface comes to consist of a macroscopically thick layer of bulk phase β . At the prewetting line, where the discontinuity in the structure of the $\alpha\gamma$ interface occurs, the two distinct surface structures may be made to coexist. The tension (excess free energy per unit length) of the boundary that separates them is the boundary tension τ_b .

There has been longstanding interest in the behavior of the line tension τ as the wetting transition is approached,^{10-16,23} i.e., in Fig. 1, as W is approached along AW; and likewise in the behavior of the boundary tension τ_b as W is approached along the prewetting line CW.^{11,14,20,21,23,24} It is well established that in mean-field approximation, with short-range forces, τ approaches a finite, positive limit, τ_w , at wetting.^{11-14,23,24} It is also known that, whatever the value τ_w of τ at the wetting transition, the boundary tension τ_b has that same limiting value as the wet-

^{a)}Corresponding author. Electronic mail: koga@cc.okayama-u.ac.jp

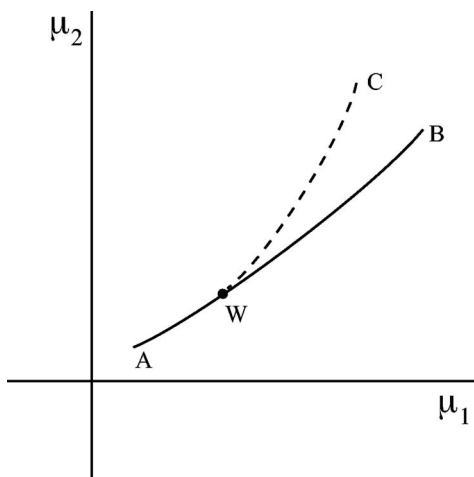


FIG. 1. Triple-point line AB and prewetting line CW projected onto the plane of two thermodynamic field variables, μ_1 and μ_2 , from the three-dimensional thermodynamic space of a two-component mixture. The wetting transition occurs at W .

ting point W is approached along the prewetting line.^{23,25,26}

Since τ_b , like a surface tension, can never be negative, it follows that τ_w is necessarily nonnegative. (In the early Ref. 25, that common limiting value τ_w for τ and τ_b was conjectured to be 0, as it was found to be in a model that later proved unrealistic, while more realistic models have since shown τ_w to be greater than 0.^{10–14,23,24})

Indekeu^{12,23} showed from an interface-displacement model that in mean-field approximation with short-range forces, the approach of τ to τ_w is of the form

$$\tau \sim \tau_w - c_1 \sqrt{b - b_w} \ln[1/(b - b_w)] \quad (b \rightarrow b_w) \quad (1)$$

where, in the notation we shall hereafter be using, b is the single independently variable thermodynamic field on the triple-point line AB in Fig. 1, and b_w is its value at the wetting transition; while c_1 is a system-dependent proportionality constant. Indekeu²³ also showed, with the same restrictions, that on the prewetting line

$$\tau_b \sim \tau_w - c_2 \sqrt{\varepsilon} \quad (\varepsilon \rightarrow 0), \quad (2)$$

with c_2 another system-dependent proportionality constant; and where ε , together with b , are the two independently variable thermodynamic fields on the $\alpha\gamma$ coexistence surface of a two-component system. The field ε in (2) has been taken to be 0 on the triple-point line, by convention. It is thus a measure of how far phase β is from coexisting with α and γ . The asymptotic formula (2) was confirmed by Varea and Robledo²⁴ in the spin-1/2 Ising model in mean-field approximation. On the prewetting line, ε and b are not independent. Hauge and Schick²² have shown that the tangency of the prewetting line to the triple-point line at $b=b_w$ in Fig. 1 is logarithmic; i.e., that on the prewetting line ε varies with b according to

$$\varepsilon \sim c_3 \frac{b_w - b}{\ln \frac{1}{b_w - b}} \quad (b \rightarrow b_w), \quad (3)$$

with c_3 now a third system-dependent proportionality constant.

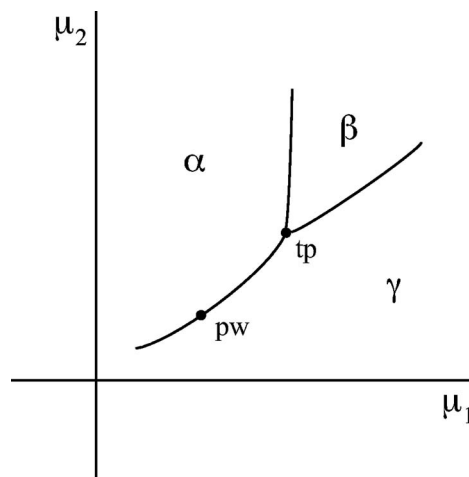


FIG. 2. Triple point tp and prewetting point pw in a one-component system. The equilibrium phases are α , β , and γ , while μ_1 and μ_2 are any two independent thermodynamic fields; e.g., any two from among the chemical potential, the pressure, and the temperature.

Our present interest is in the status of Eqs. (1)–(3) in a particular mean-field density-functional model, but we may note in passing the simpler picture one has in a one-component system, illustrated in Fig. 2. The thermodynamic space is now two dimensional, and the triple point and possible prewetting point are now single, isolated points, not lines of points. In the figure, μ_1 and μ_2 are any two independent field variables; e.g., any two from among the chemical potential, the pressure, and the temperature. At the triple point tp one of the phases may or may not wet the interface between the other two. If β , say, does wet the $\alpha\gamma$ interface at the triple point, then in all the nearby two-phase $\alpha\gamma$ states the $\alpha\gamma$ interface will consist of a β -like layer that gradually thickens to a macroscopically thick bulk β at the triple point itself. If α and γ are a solid and its vapor, and β the melt, the phenomenon is termed premelting. In mean-field approximation, with short-range forces, the layer thickens proportionally to the logarithm of the distance from the triple point;²⁷ i.e., as $\ln(1/\varepsilon)$, in our present notation. [With the same assumptions, the same law of growth of the wetting layer holds on approach to any point on the triple-point line WB in Fig. 1.²⁷ The logarithm in (3) is a manifestation of this logarithmic wetting-layer growth.²²] A logarithmic growth of the wetting layer thickness has been observed on those facets of crystalline lead that premelt.²⁸ It is likely that ordinary ice premelts,²⁹ but that may depend on the presence of impurities³⁰ and may depend also on what facet of the crystal is exposed to the vapor. When, in Fig. 2, β wets the $\alpha\gamma$ interface at the triple point, there may then also be a prewetting point, marked pw on the $\alpha\gamma$ equilibrium line in the figure, such that in states on the $\alpha\gamma$ line further from the triple point than pw there is no premonitory β -like layer in the $\alpha\gamma$ interface. The β -like layer then appears suddenly at pw . Only at pw is there a boundary tension τ_b and only at tp can there be a line tension τ , but there cannot be both a τ_b and a τ in the system pictured in Fig. 2: if there is a prewetting point pw with its associated τ_b then the system is wetting at tp , in which case there is no τ , whereas if the system is nonwet at tp , so there is a τ , then there is no prewetting

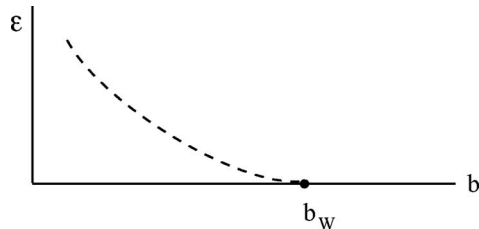


FIG. 3. The triple-point line is the b axis ($\varepsilon=0$). The prewetting line is the dashed curve, which meets the b axis at the wetting transition, where $b=b_w$.

point p_w . That is the reason our present study is with a system like that in Fig. 1 and not with one like that in Fig. 2.

A mean-field density-functional model that has often been called on to illustrate numerically the asymptotic behavior in Eqs. (1)–(3) has typically been frustrated by insufficient numerical precision,^{10,20,31} especially because of the great precision required to establish unambiguously the presence of logarithmic factors. We have now largely overcome these difficulties, and we here report the results of the most recent numerical study of the model, which we hope will provide benchmarks for later work. We believe we have convincingly established the asymptotic formulas (1)–(3) for the model, in gratifying agreement with theory, as well as the principle of the equality of τ and τ_b at wetting, again in agreement with theory.

In the next section we recall the model, which occurs in two versions, one with $\varepsilon=0$, for the study of the line tension τ in three-phase equilibrium,^{10,31} and one with a prewetting line on which $\varepsilon \neq 0$, for the study of the boundary tension τ_b .²⁰ The first of those has also been used for the purpose of establishing an adsorption equation for the contact line analogous to the Gibbs adsorption equation for interfaces,^{32,33} but that is not our present concern. As a by-product of the study, in the model's fully symmetric three-phase state, far from wetting, it is found that certain properties of the model's line tension and densities are almost surely given by simple numbers arising from the symmetries, but proving that these are exact for the model remains a challenge to analytical theory.

The model in its two versions is recalled in the following section, the numerical methods and results are given in Sec. III, and the results are briefly summarized in the concluding Sec. IV.

II. THE MODEL RECALLED

The density functional to be treated has two thermodynamic field variables, b and ε . The b, ε plane (analogous to the μ_1, μ_2 plane in Fig. 1) is pictured schematically in Fig. 3. The triple-point line is the b axis, so its equation is $\varepsilon=0$. On that line, three phases, α, β, γ , may coexist. Wherever $\varepsilon > 0$, only the phases α and γ may coexist, so ε is a measure of how far the thermodynamic state is from one in which β could be stable as a macroscopic phase in equilibrium with α and γ . The prewetting line meets the triple-point line at $\varepsilon=0, b=b_w$, which is where the wetting transition occurs (the point W in Fig. 1).

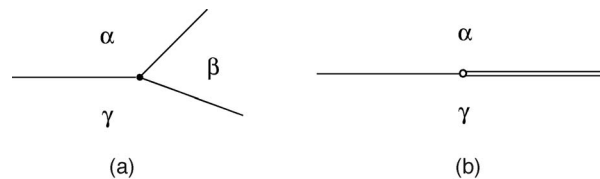


FIG. 4. (a) Three phases α, β, γ occupying the dihedral angles between planar interfaces. The three-phase contact line, marked by a dot, and the interfaces, are perpendicular to the plane of the figure. (b) Two distinct surface phases coexisting in the $\alpha\gamma$ interface. The boundary between the surface phases, marked by a small circle, and the $\alpha\gamma$ interface, are perpendicular to the plane of the figure.

The physical space occupied by the equilibrium phases is pictured schematically in Fig. 4. In Fig. 4(a), the three phases α, β, γ coexist. The three-phase contact line is perpendicular to the plane of the figure, as are the three interfaces. The three phases occupy the dihedral angles between surface planes. The contact “line” and surface “planes” have diffuse structures on a molecular scale. The structure and composition of the system vary only in the plane of the figure; they are uniform in the direction of the contact line. As b approaches b_w at the wetting transition, the contact angle β closes down to 0. At prewetting, two distinct surface structures may coexist in the $\alpha\gamma$ interface with a boundary line (again a diffuse region) separating them. This is shown in Fig. 4(b), where the $\alpha\gamma$ interface and the boundary line between its two surface structures are perpendicular to the plane of the figure. As the point in Fig. 3 that represents the state of the system moves along the b axis with decreasing b to b_w and then onto the prewetting line, the phase equilibrium depicted in Fig. 4(a) changes continuously into that in Fig. 4(b), the contact line in 4(a) transforming continuously into the boundary line in 4(b). It is because of this continuous transformation that the line tension τ and boundary tension τ_b have equal values at the wetting transition.^{23,25,26}

The model free-energy density Ψ is now taken to be of the form

$$\Psi = F(\rho_1, \rho_2; b, \varepsilon) + \frac{1}{2}(|\nabla\rho_1|^2 + |\nabla\rho_2|^2) \quad (4)$$

where $\rho_1(\mathbf{r})$ and $\rho_2(\mathbf{r})$ are two density or composition variables that vary with position \mathbf{r} in the plane of Fig. 4 and ∇ is the two-dimensional gradient operator in the plane. Specifically, the function F is taken to be²⁰

$$F(\rho_1, \rho_2; b, \varepsilon) = 16\rho_2^2(\rho_2 - b)^2 + [(\rho_2 - b\rho_1)^2 - b^2]^2 + [(\rho_2 + b\rho_1)^2 - b^2]^2 + \varepsilon(\rho_1^2 - 1)^2. \quad (5)$$

This is always positive except at the compositions of the bulk phases, where it is 0. In the α and γ phases,

$$\rho_1 = -1, \quad \rho_2 = 0 \quad (\text{phase } \alpha); \quad (6)$$

$$\rho_1 = 1, \quad \rho_2 = 0 \quad (\text{phase } \gamma).$$

When $\varepsilon \neq 0$, these are the only phases that may be present and the only conditions under which $F=0$; but when $\varepsilon=0$ the β phase, of composition

$$\rho_1 = 0, \quad \rho_2 = b \quad (\text{phase } \beta, \text{ when } \varepsilon=0), \quad (7)$$

may coexist with α and γ , and $F=0$ there also.

Far from the contact line the spatial structures vary only in the directions perpendicular to the interfaces. For each of the three interfaces in the three-phase equilibrium ($\varepsilon=0$), or for the $\alpha\gamma$ interface alone in the two-phase equilibrium ($\varepsilon>0$), call that direction z . The corresponding interfacial tension, for example $\sigma_{\alpha\gamma}$ is then found by variationally minimizing the integral of Ψ with respect to the densities ρ_1 and ρ_2 , which are then functions only of z ,

$$\sigma_{\alpha\gamma} = \min_{\rho_1, \rho_2} \int_{-\infty}^{\infty} \Psi dz, \quad (8)$$

and similarly for $\sigma_{\alpha\beta}$ and $\sigma_{\beta\gamma}$ (By symmetry, $\sigma_{\alpha\beta} = \sigma_{\beta\gamma}$). The integrals for the several interfaces differ in the prescribed boundary values of ρ_1 and ρ_2 at $z = \pm\infty$, as given by (6) and (7). The Euler-Lagrange equations corresponding to the minimizations in (8) are

$$d^2\rho_1/dz^2 = \partial F/\partial\rho_1, \quad d^2\rho_2/dz^2 = \partial F/\partial\rho_2, \quad (9)$$

and are to be solved subject, again, to the prescribed boundary values of ρ_1 and ρ_2 at $z = \pm\infty$.

There are always two solutions of (9) for the $\alpha\gamma$ interface, one corresponding to the interface wet by bulk-phase β or prewet by a β -like layer, and the other not wet or prewet. For the latter one has analytically the solution²⁰

$$\rho_1 = \tanh(z/2\xi), \quad \rho_2 \equiv 0 \quad (10)$$

where

$$\xi = \frac{1}{4(b^4 + \frac{1}{2}\varepsilon)^{1/2}}, \quad (11)$$

and with the corresponding tension, call it $\sigma_{\alpha\gamma}^*$ calculated as $\int_{-\infty}^{\infty} \Psi dz$ with the ρ_1, ρ_2 of (10),

$$\sigma_{\alpha\gamma}^* = \frac{8}{3}(b^4 + \frac{1}{2}\varepsilon)^{1/2}. \quad (12)$$

The second solution of (9) for the $\alpha\gamma$ interface is the one in which it is wet or prewet by β , when $\varepsilon=0$ or $\varepsilon>0$, respectively. In that solution one has $\rho_1=0$ in the middle of the $\alpha\gamma$ interface and either $\rho_2=b$ (wetting) or $\rho_2 \simeq b$ (prewetting) there, while far from the middle the structure is like that of an $\alpha\beta$ interface on one side and a $\beta\gamma$ interface on the other. The associated tension, call it $\sigma_{\alpha\gamma}^{**}$ is again calculated as $\int_{-\infty}^{\infty} \Psi dz$, now with this ρ_1, ρ_2 . In the case of three-phase equilibrium, which can occur only with $\varepsilon=0$, one has $\sigma_{\alpha\gamma}^{**} = \sigma_{\alpha\beta} + \sigma_{\beta\gamma}$.

When $\sigma_{\alpha\gamma}^* < \sigma_{\alpha\gamma}^{**}$ the $\alpha\gamma$ interface's stable structure is the nonwet or nonprewet one, with $\sigma_{\alpha\gamma} = \sigma_{\alpha\gamma}^*$ while when $\sigma_{\alpha\gamma}^* > \sigma_{\alpha\gamma}^{**}$ the stable structure is the wet or prewet one, with $\sigma_{\alpha\gamma} = \sigma_{\alpha\gamma}^{**}$. The wetting and prewetting transitions, with $\varepsilon=0$ and $\varepsilon>0$, respectively, occur when $\sigma_{\alpha\gamma}^* = \sigma_{\alpha\gamma}^{**}$. When $\varepsilon=0$, one has $\sigma_{\alpha\gamma}^* = \frac{8}{3}b^2$, by (12), while $\sigma_{\alpha\gamma}^{**} = \sigma_{\alpha\beta} + \sigma_{\beta\gamma}$ and both are functions only of b ; so b_w , the value of b at wetting, is found as the solution of

$$\sigma_{\alpha\gamma}^* = \sigma_{\alpha\beta} + \sigma_{\beta\gamma} \quad (\text{wetting transition, } \varepsilon=0), \quad (13)$$

with $\sigma_{\alpha\gamma}^* = \frac{8}{3}b^2$, and with $\sigma_{\alpha\beta} = \sigma_{\beta\gamma}$ still, by symmetry. When $\varepsilon>0$, the two tensions $\sigma_{\alpha\gamma}^*$ and $\sigma_{\alpha\gamma}^{**}$ are functions of both ε and b , and the equation of the prewetting line in the b, ε plane is then²⁰

$$\sigma_{\alpha\gamma}^* = \sigma_{\alpha\gamma}^{**} \quad (\text{prewetting line in } b, \varepsilon \text{ plane}), \quad (14)$$

with $\sigma_{\alpha\gamma}^*$ given by (12).

To calculate the line tension τ at an $\alpha\beta\gamma$ triple point ($\varepsilon=0$), choose and fix a point in the plane of Fig. 4(a) to be the nominal location of the contact line (the dot in the figure), and construct around that point a large triangle (Neumann triangle) with sides perpendicular to the three interfaces and distant $R_{\alpha\beta}, R_{\beta\gamma}, R_{\alpha\gamma}$ from the chosen point. These $R_{\alpha\beta}$, etc., are to be taken sufficiently large so that ρ_1 and ρ_2 along the sides of the triangle are effectively identical with what they are in the interfaces infinitely far from the contact line. Then

$$\tau = \lim_{R_{\alpha\beta} \rightarrow \infty, \text{etc.}} \left[\min_{\rho_1, \rho_2} \int_A \Psi da - (\sigma_{\alpha\beta} R_{\alpha\beta} + \sigma_{\beta\gamma} R_{\beta\gamma} + \sigma_{\alpha\gamma} R_{\alpha\gamma}) \right], \quad (15)$$

where the integration is through the area A of the triangle with da an element of area. The $\sigma_{\alpha\gamma}$ in (15) is $\sigma_{\alpha\gamma}^* = \frac{8}{3}b^2$, the tension of the nonwet $\alpha\gamma$ interface. The variational minimization over ρ_1 and ρ_2 in (15) is done with ρ_1 and ρ_2 on the sides of the triangle specified to be the respective interfacial profiles $\rho_1(z)$ and $\rho_2(z)$, and the minimization then determines $\rho_1(\mathbf{r})$ and $\rho_2(\mathbf{r})$ in the interior of the triangle. Equivalently, $\rho_1(\mathbf{r})$ and $\rho_2(\mathbf{r})$ may be obtained as solutions of the Euler-Lagrange equations

$$\nabla^2\rho_1 = \partial F/\partial\rho_1, \quad \nabla^2\rho_2 = \partial F/\partial\rho_2 \quad (16)$$

subject to the same boundary conditions. For the numerical solution, it is more convenient to apply the boundary conditions on the sides of a large rectangle with sides parallel and perpendicular to the $\alpha\gamma$ interface than on the sides of the Neumann triangle.³² Once $\rho_1(\mathbf{r})$ and $\rho_2(\mathbf{r})$ are determined, τ may be found from (15) itself, or, alternatively, and with greater numerical precision, from the Kerins-Boiteux integral³⁴

$$\tau = \int_A (\Psi - 2F) da. \quad (17)$$

The integrand in (17), unlike that in (15), is short ranged.

For the boundary tension τ_b , with ε in (5) positive, the spatial structure is now like that in Fig. 4(b). One may define an x, z coordinate system in the plane of the figure, with origin at the boundary between the surface phases (the small circle in the figure), and with the x axis parallel to the plane of the $\alpha\gamma$ interface and the z axis perpendicular to it. Then²⁰

$$\tau_b = \min_{\rho_1, \rho_2} \int_{-\infty}^{\infty} \left(\int_{-\infty}^{\infty} \Psi dz - \sigma_{\alpha\gamma} \right) dx, \quad (18)$$

with $\sigma_{\alpha\gamma}$ now the common value of $\sigma_{\alpha\gamma}^*$ and $\sigma_{\alpha\gamma}^{**}$ at prewetting; viz., $\frac{8}{3}(b^4 + \frac{1}{2}\varepsilon)^{1/2}$. The variational minimization over ρ_1 and ρ_2 in (18) is done with ρ_1 and ρ_2 specified to have their bulk α - and γ -phase values as $z \rightarrow \pm\infty$ for any fixed x and to be identical with the corresponding interfacial profiles $\rho_1(z)$ and $\rho_2(z)$ of the nonprewet or prewet interfaces as $x \rightarrow \pm\infty$ for any fixed z . Equivalently, $\rho_1(\mathbf{r})$ and $\rho_2(\mathbf{r})$ may be obtained from the Euler-Lagrange equations (17) subject to

those boundary conditions. Once $\rho_1(\mathbf{r})$ and $\rho_2(\mathbf{r})$ are determined, τ_b may be calculated from (18) itself, or, alternatively, and with greater numerical precision, from the Kerins-Boiteux integral, which is now^{14,21}

$$\tau_b = \int_{-\infty}^{\infty} \int_{-\infty}^{\infty} (\Psi - 2F) dz dx. \quad (19)$$

The model, and the formulas and principles for the location of the wetting and prewetting transitions and the calculation of the line and boundary tensions, have now been recalled. In the next section we describe the numerical implementation and results.

III. NUMERICAL METHODS AND RESULTS

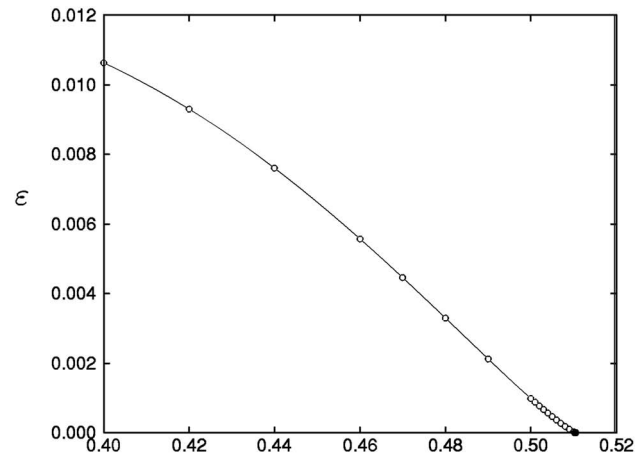
The asymptotic behavior of τ and τ_b on approach to wetting is obtained from a series of numerical calculations: first, b_w , the value of b at wetting; second, the points (b, ε) on the prewetting line; third, the interfacial profiles $\rho_1(z)$ and $\rho_2(z)$ infinitely far from the contact line ($b > b_w$) or the boundary line ($b < b_w$); and fourth, the density profiles $\rho_1(\mathbf{r})$ and $\rho_2(\mathbf{r})$ in a rectangular area that includes three or two distinct interfaces in contact. Each step must be made with great numerical accuracy in order that the final results bear comparison with the asymptotic forms (1)–(3), including the logarithmic factors in (1) and (3).

In the numerical calculations of $\rho_1(z)$ and $\rho_2(z)$ we discretize the Euler-Lagrange equations with a five-point difference equation in z , and then solve them iteratively with a successive over-relaxation (SOR) method.³⁵ The range $[-z_{\max}, z_{\max}]$ and the grid spacing Δz necessary for the equations to be solved accurately depend on b and ε : for example, along the triple-point line $z_{\max} = 3$ and $\Delta z = 0.003$ are sufficient for the symmetric case $b = \sqrt{3}$, while $z_{\max} = 30$ is necessary for $b \approx b_w$, whereas $\Delta z = 0.02$ is then sufficient because the profiles are then less rapidly varying. The values of ρ_1 and ρ_2 at the end points of the range of z are fixed to those of the bulk phases. The initial guesses of $\rho_1(z)$ and $\rho_2(z)$ are taken to be a step function with two intervals, $[-z_{\max}, 0)$ and $[0, z_{\max}]$, for the interfaces that are not wet or prewet, and a step function with three intervals, $[-z_{\max}, -z_\beta)$, $[-z_\beta, z_\beta]$, $(z_\beta, z_{\max}]$, where the values in the middle interval are taken to be those of the bulk β phase and where a value of z_β suitable for the resulting interface to be the $\alpha\gamma$ interface prewet by β depends on b and ε . The criterion for convergence is an rms difference of less than 1×10^{-13} between iterates. As a test of the numerical precision, solutions are obtained for the $\alpha\gamma$ interface, too. Then the numerical profiles exactly coincide with the analytical profiles (10) and the value of $\sigma_{\alpha\gamma}^*$ is accurate to eight digits as compared against the analytical result (12).

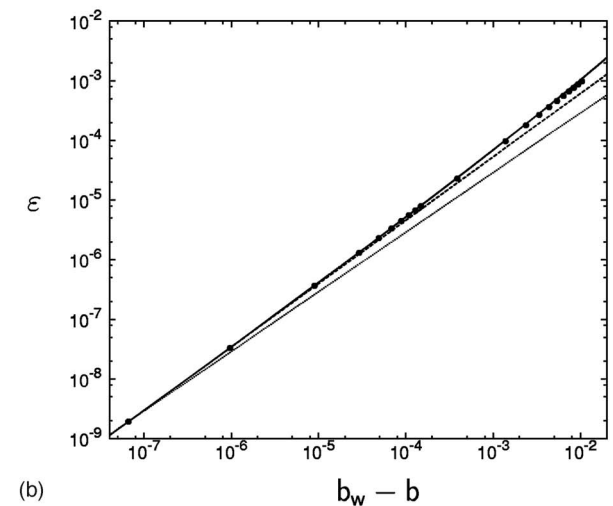
As the solution of Eq. (13), the value of b at wetting is found to be

$$b_w = 0.510\,388\,966\dots, \quad (20)$$

for which $|\sigma_{\alpha\gamma}^* - \sigma_{\alpha\beta} - \sigma_{\beta\gamma}| < 10^{-10}$. Likewise, the points (b, ε) on the prewetting line are obtained as the solution of Eq. (14): in practice, for each given b , we repeat the calculation of $\sigma_{\alpha\gamma}^*$ and $\sigma_{\alpha\gamma}^{**}$ with changing ε until the criterion



(a)



(b)

FIG. 5. (a) The points (b, ε) on the prewetting line. Open circles represent the numerical results and the filled circle on the b axis indicates b_w . (b) Logarithmic plots of ε vs $b_w - b$ on the prewetting line. The solid curve is $c_3(b_w - b) / \ln[1/(b_w - b)]$ with $c_3 = 0.479\,91$, the dashed line is $c(b_w - b)^\alpha$ with $c = 0.082\,24$, $\alpha = 1.062\,99$, and the dotted line is $c(b_w - b)$ with $c = 2.9036$. The points are the numerical results.

$|\sigma_{\alpha\gamma}^* - \sigma_{\alpha\gamma}^{**}| < 10^{-10}$ is satisfied. The line of prewetting transitions as so determined is shown in Fig. 5. The curve in Fig. 5(a) is basically the same as that in Fig. 3 in Ref. 20; the difference is that data points are now extended toward the wetting transition much more closely than before, the closest being at $b_w - b < 10^{-7}$. As remarked in the earlier study,²⁰ there is no indication in Fig. 5(a) that the prewetting line meets the b axis tangentially at b_w in the b, ε plane. But one can see the tangency in the logarithmic plot of ε versus $b_w - b$ in Fig. 5(b). Plotted together with the data points are fits of $c(b_w - b)$, of $c(b_w - b)^\alpha$, and of the predicted form $c_3(b_w - b) / \ln[1/(b_w - b)]$. The function $c(b_w - b)^\alpha$ with $\alpha = 1.062\,99$ and $c = 0.082\,24$ [the dashed line in Fig. 5(b)] fits the data better than $c(b_w - b)$ with $c = 2.9036$ (the dotted line). This alone indicates that the prewetting line meets the b axis tangentially. A more important fact is that the data are fit by $c_3(b_w - b) / \ln[1/(b_w - b)]$ with $c_3 = 0.479\,91$ extremely well, even better than by $c(b_w - b)^\alpha$. That is, the numerical results support the presence of the logarithm in (3).

Equilibrium densities $\rho_1(\mathbf{r})$ and $\rho_2(\mathbf{r})$ over a rectangular

TABLE I. Conditions for the numerical calculation of $\rho_1(\mathbf{r})$ and $\rho_2(\mathbf{r})$. The values of Δy in parentheses are those used in preparatory calculations.

b	$\beta(^{\circ})$	box size ($L_x \times L_y$)	grid spacing Δx	Δy
$\sqrt{3}$	120	3×3	0.003	0.003
0.518	12.1	24×96	0.024	0.024(0.24)
0.5105	1.47	40×800	0.02	0.10(0.8)
0.510	0	40×400	0.02	0.02(0.4)
0.506	0	40×200	0.02	0.02(0.4)

box that includes the three phases in contact or two surface phases in contact are obtained as solutions of the two-dimensional Euler-Lagrange equations (16) subject to the boundary conditions on the sides of the rectangle with sides parallel and perpendicular to the $\alpha\gamma$ interface. The Euler-Lagrange equations are discretized with a nine-point stencil over the rectangular box and then are solved iteratively with the SOR method.³⁵ With $\rho_1(\mathbf{r})$ and $\rho_2(\mathbf{r})$ as so obtained, the line tension τ (for $b > b_w$) and the boundary tension τ_b (for $b < b_w$) are evaluated from the Kerins-Boiteux integrals (17) and (19), rather than the general expressions (15) and (18). It has long been recognized that the numerical calculation of τ becomes harder on approach to wetting. One reason is that the region, now a rectangular box, that includes the inhomogeneity due to the three phases in contact expands in area rapidly as b approaches b_w in the vicinity of wetting. Another reason is that convergence to the equilibrium densities becomes slower as b approaches b_w . These two together inexorably increase the computation time for solving the Euler-Lagrange equations on approach to wetting. The same is true for the numerical calculation of τ_b . But it is of critical importance for our purpose, which is to examine the behaviors of τ and τ_b on approach to wetting, that the region be taken sufficiently large and that the convergence criterion be as strict as in the calculation in states far from wetting. To make the computation tractable while satisfying those two conditions, the sides L_x and L_y of the rectangular box and the grid spacings Δx and Δy in the directions perpendicular and parallel to the $\alpha\gamma$ interface, respectively, are chosen to be values appropriate for each b . When b is very close to b_w , an additional strategy is necessary for keeping the computation time realistic: minimization of $\int \Psi da$ for a given grid and interpo-

lation of the resulting ρ_1 and ρ_2 to a finer grid are repeated until the results become independent of the grid spacing. In addition, a parallel computation algorithm is combined with quad-core 3.0 GHz Intel Xeon processors. Without these strategies and the high-performance computer it would be impossible to achieve the great precision required to establish the formulas (1) and (3) for the model, at least within a practical time period. The rectangular box sizes and the grid spacings employed for representative calculations are given in Table I. The criterion for convergence was an rms difference in ρ_1 and ρ_2 of less than 1×10^{-10} between iterates. Near the wetting transition it required up to two weeks of continuous operation before this criterion was satisfied.

The contact angle β in Table I was calculated from⁵

$$\cos \beta = 1 - \frac{(\sigma_{\alpha\beta} + \sigma_{\beta\gamma} - \sigma_{\alpha\gamma})(\sigma_{\alpha\beta} + \sigma_{\beta\gamma} + \sigma_{\alpha\gamma})}{2\sigma_{\alpha\beta}\sigma_{\beta\gamma}}. \quad (21)$$

The behavior of τ near wetting is shown in Fig. 6. When τ at the three values of b closest to b_w are plotted against $\sqrt{b-b_w}$ [Fig. 6(a)], it is clear that the points do not lie on a straight line and that the limiting value τ_w is not determined by linear extrapolation of this plot. But when the same values of τ are plotted against $\sqrt{b-b_w} \ln[1/(b-b_w)]$ [Fig. 6(b)], the points do lie on a straight line and may be reliably extrapolated to a limiting value as b goes to b_w . This is strong evidence for the presence of the logarithmic factor in Eq. (1). Let the three data points closest to wetting be numbered 1, 2, 3 with 1 the closest. Then linear fits to the pairs of points (1, 2), (1, 3), and (2, 3) give τ_w , the limiting value of τ at wetting, to be 0.492 05, 0.492 15, and 0.492 26, respectively, while the coefficient c_1 in (1) is 0.4549, 0.4559, and 0.4564, respectively.

Figure 7 shows the boundary tension τ_b as a function of ε . It is clear that τ_b varies linearly with $\sqrt{\varepsilon}$ for ε close to 0, which is the behavior (2) predicted by theory. We find the coefficient c_2 in (2) to be 2.729. With both (3) and (2) confirmed for this model, we find another logarithmic factor in the behavior of τ_b against $b_w - b$:

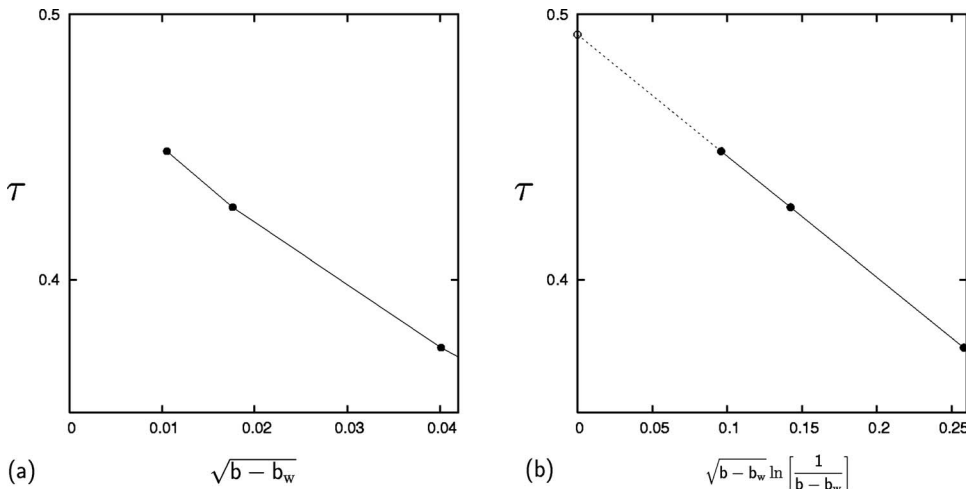


FIG. 6. (a) τ vs $\sqrt{b-b_w}$. (b) τ vs $\sqrt{b-b_w} \ln[1/(b-b_w)]$. The dotted line in (b) is a linear extension of the plot and the open circle indicates the extrapolated value of τ for $b=b_w$.

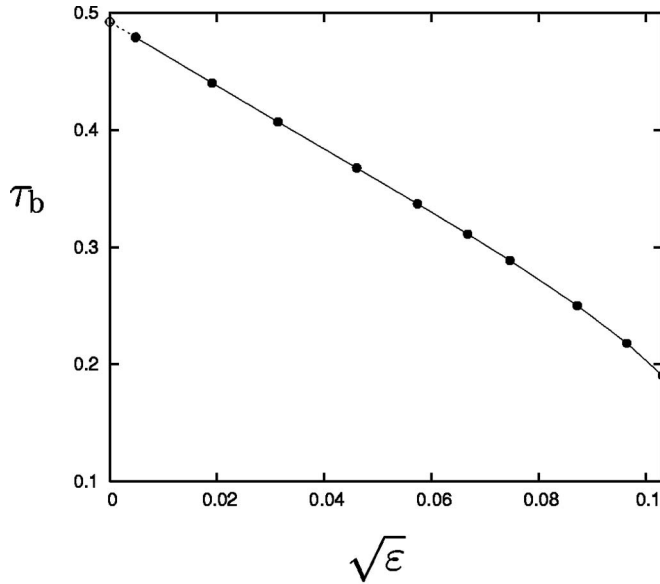


FIG. 7. τ_b vs $\sqrt{\varepsilon}$. The dotted line is a linear extension of the plot and the open circle indicates the extrapolated value of τ_b for $b=b_w$.

$$\tau_b \sim \tau_w - c_4 \sqrt{\frac{b_w - b}{\ln\left[\frac{1}{b_w - b}\right]}} \quad (22)$$

where $c_4 = c_2 \sqrt{c_3} = 1.8905$. The fit to the two data points (τ_b , $\sqrt{\varepsilon}$) closest to the wetting transition gives 0.492 37 as the value of τ_w in (2). Since this value is essentially the same as the limiting value obtained from the data points of τ versus $\sqrt{b-b_w} \ln[1/(b-b_w)]$ in Fig. 6(b), it has now been demonstrated that the boundary tension and the line tension have a common limiting value at the wetting transition. The common value for the model is determined to three decimal places:

$$\tau_w = 0.492. \quad (23)$$

The much higher values seen earlier^{10,31} were probably a result of inaccuracies in the numerically calculated densities, which would then have yielded only a variational upper bound to τ_w . Together with the present τ_w , the numerical results for τ and τ_b are now plotted over a wide range of b including the vicinity of the wetting transition, as shown in Fig. 8. The behavior of the boundary tension τ_b and the line tension τ are now accurately determined: the cusp in the composite plot is asymptotically of the form (1) for $b > b_w$ and of the form (22) for $b < b_w$, while τ and τ_b converge to the common limiting value τ_w .

With the numerical values $c_4 = 1.8905$ and $c_1 = 0.455$ found above, we have $c_4/c_1 = 4.15$, to be compared with the 5.515 found for this quantity by Robledo and Indekeu¹³ as a universal amplitude ratio. Because the amplitudes of terms with logarithmic factors are always difficult to assess accurately, and the effects of correction terms to the leading asymptotic behavior is not known, this may be taken for now as satisfactory agreement.

It was remarked earlier that it is expected that the thickness of the β -like layer in the prewet $\alpha\gamma$ interface would increase proportionally to $\ln(1/\varepsilon)$ as the triple-point line was approached²⁷ [$\varepsilon \rightarrow 0$ at fixed $b < b_w$ in Fig. 5(a)], or as the

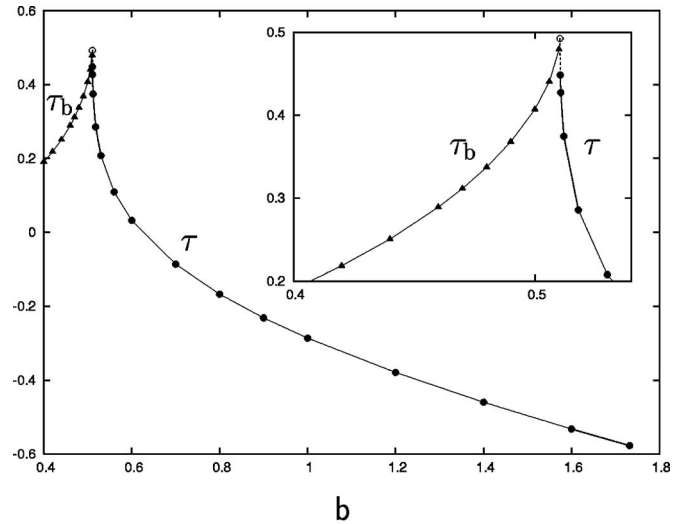


FIG. 8. Line tension τ and boundary tension τ_b as functions of b . The open circle indicates the common limiting value $\tau_w = 0.492$ at wetting.

bulk wetting transition was approached along the prewetting line.²² The density $\rho_1(z)$ in the prewet $\alpha\gamma$ interface, with $z=0$ taken to be the point about which $\rho_1(z)$ is antisymmetric, has a nearly horizontal plateau corresponding to the slowly varying $\rho_1 \approx 0$ in the β -like layer. This nearly flat portion of $\rho_1(z)$ lies between two points of inflection, the distance ℓ between which may be taken as a measure of the thickness of the wetting layer.²⁷ In Fig. 9 is plotted ℓ versus $\ln(1/\varepsilon)$, where one does indeed see the logarithmic growth on approach to the wetting transition; it is accurately logarithmic for $\varepsilon < 10^{-5}$.

As a by-product of these calculations, requiring the same numerical precision, are properties of the model in its fully symmetric state, $b = \sqrt{3}$, which is far from the wetting transition at $b = b_w$. Here the three phases α, β, γ play symmetrical roles in the phase equilibrium and all the contact angles in Fig. 4(a) are 120° . It was already reported for this model³³

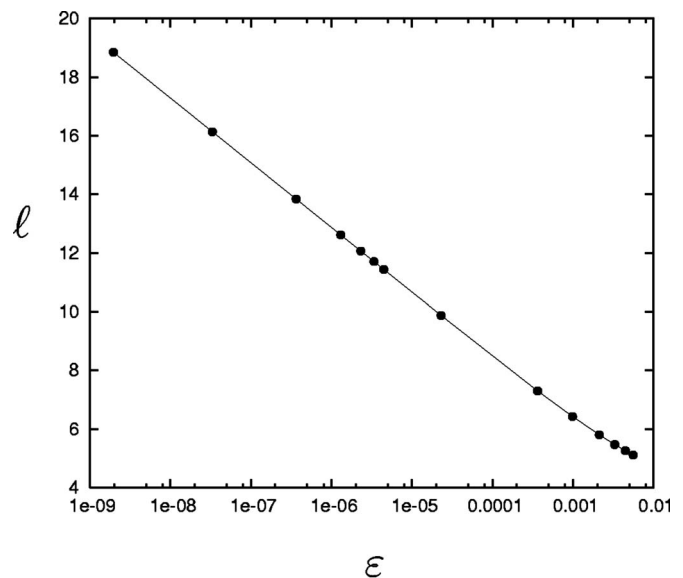


FIG. 9. Thickness ℓ of the β -like layer in the prewet $\alpha\gamma$ interface as a function of ε on the prewetting line. The ε scale is logarithmic.

that in this fully symmetric case $\tau = -0.577\ 349$ and $d\tau/db = -0.333\ 353$ or $-0.333\ 344$. It was then conjectured that because of the ubiquitous appearance of the numbers 3 and $\sqrt{3}$ in this symmetric case, these are exactly

$$\tau_{b=\sqrt{3}} = -\frac{1}{\sqrt{3}} = -0.577\ 350\ 269 \dots, \quad (24)$$

$$\left. \frac{d\tau}{db} \right|_{b=\sqrt{3}} = -\frac{1}{3} = -0.333\ 333\ 333 \dots. \quad (25)$$

We now note another striking numerical coincidence in this symmetric case. With all the contact angles in Fig. 4(a) now 120° , introduce polar coordinates r, θ with origin at the symmetry point of the phase equilibrium and θ measured from a polar axis that is taken to be the extension of the $\alpha\gamma$ interface bisecting the contact angle β . It is then a known consequence of the symmetry¹⁰ that $\rho_1 \sim Ar \sin \theta$ and $\rho_2 - 1/\sqrt{3} \sim Ar \cos \theta$, asymptotically as $r \rightarrow 0$, with the same coefficient A in both. The present numerical calculations yield values of A from 3.999 997 2 to 4.000 000 6, with the obvious conjecture that

$$A = 4. \quad (26)$$

Proving that (24)–(26) are exact for the model in the symmetric case $b = \sqrt{3}$ remains a challenge to analytical theory.

IV. SUMMARY

For a mean-field density-functional model of line tension that had been frequently studied in the past, we have obtained numerically precise accounts of the behavior on approach to a wetting transition of both the line tension τ in three-phase α, β, γ equilibrium and the boundary tension τ_b between two coexisting surface phases in the $\alpha\gamma$ interface. The model has two variable thermodynamic fields, ε and b , with $\varepsilon = 0$ in the three-phase equilibrium. Only phases α and γ are present as bulk phases when $\varepsilon > 0$. The wetting transition, between states in which the β phase does and does not wet the $\alpha\gamma$ interface, occurs at $\varepsilon = 0$, $b = b_w$. There is a prewetting line in the ε, b plane [Fig. 5(a)], such that in states ε, b above that line the $\alpha\gamma$ interface is not prewet by a β -like layer while in states below the line it is. On the prewetting line itself the two distinct structures of the $\alpha\gamma$ interface may coexist with boundary tension τ_b . The line tension τ is calculated for the three-phase states $\varepsilon = 0$, $b > b_w$, and τ_b for states on the prewetting line at $b < b_w$.

It is well established that in mean-field approximation, with short-range forces, τ should approach a finite positive limit, τ_w , at wetting.^{11–14,23,24} It is also known that, whatever the value τ_w of τ at the wetting transition, the boundary tension τ_b should have that same limiting value as the wetting-transition point is approached along the prewetting line.^{23,25,26} Indekeu^{12,23} had shown from an interface displacement model that in mean-field approximation, with short-range forces, τ would approach τ_w as in (1) and that, with the same restrictions,²³ τ_b on the prewetting line would approach τ_w as in (2). Hauge and Schick²² showed that ε as a function of b on the prewetting line, in the asymptotic limit $b \rightarrow b_w$, would be given by (3). The main purpose of this

paper was to establish convincingly, especially with sufficient numerical accuracy to display the logarithmic factors, that (1)–(3) hold for the density-functional model treated here, and also that τ and τ_b in the model share a common limiting value τ_w . These facts have been demonstrated with the results given in Sec. III and displayed in Figs. 5(b), 6(b), 7, and 8. It was also noted that the thickness ℓ of the β -like layer in the $\alpha\gamma$ interface is expected to increase proportionally to $\ln(1/\varepsilon)$ as $\varepsilon \rightarrow 0$ along the prewetting line,²² and this is accurately confirmed for the model with the numerical results displayed in Fig. 9.

When the properties of the model are obtained with the same numerical precision in the fully symmetric three-phase equilibrium, where $b = \sqrt{3}$, far from the wetting transition, one finds with near certainty the results in (24)–(26), but it remains as a challenge to prove they are exact by deriving them analytically.

ACKNOWLEDGMENTS

We thank J. O. Indekeu for helpful comments that have been incorporated in the paper. K.K. acknowledges support by the MEXT Grant-in-Aid for Scientific Research and NAREGI. B.W. acknowledges support by the U.S. National Science Foundation.

- ¹S. Dietrich, in *Phase Transitions and Critical Phenomena*, edited by C. Domb and J. L. Lebowitz (Academic Press, New York, 1988), Chap. 1, Vol. 12, pp. 1–218.
- ²M. Schick, *Introduction to Wetting Phenomena, Course 9 in Liquides aux interfaces/Liquids at Interfaces, Les Houches, Session XLVIII, 1988*, edited by J. Charvolin, J. F. Joanny, and J. Zinn-Justin (Elsevier, New York, 1990).
- ³J. O. Indekeu, *Acta Phys. Pol. B* **26**, 1065 (1995).
- ⁴E. M. Blokhuis and B. Widom, *Curr. Opin. Colloid Interface Sci.* **1**, 424 (1996).
- ⁵J. S. Rowlinson and B. Widom, *Molecular Theory of Capillarity* (Oxford University Press, Oxford, 1982), Chap. 8.
- ⁶A. Winter, *Heterog. Chem. Rev.* **2**, 269 (1995).
- ⁷J. W. Gibbs, *The Collected Works of J. Willard Gibbs* (Longmans, Green, New York, 1928), Vol. 1, p. 288 (footnote).
- ⁸P. G. de Gennes, F. Brochard-Wyart, and D. Quéré, *Capillarity and Wetting Phenomena: Drops, Bubbles, Pearls, Waves* (Springer, New York, 2004), pp. 72–73.
- ⁹B. V. Toshev, D. Platikanov, and A. Scheludko, *Langmuir* **4**, 489 (1988).
- ¹⁰I. Szeleifer and B. Widom, *Mol. Phys.* **75**, 925 (1992).
- ¹¹E. M. Blokhuis, *Physica A* **202**, 402 (1994).
- ¹²J. O. Indekeu, *Int. J. Mod. Phys. B* **8**, 309 (1994).
- ¹³A. Robledo and J. O. Indekeu, *Europhys. Lett.* **25**, 17 (1994).
- ¹⁴S. Perković, E. M. Blokhuis, and G. Han, *J. Chem. Phys.* **102**, 400 (1995).
- ¹⁵T. Getta and S. Dietrich, *Phys. Rev. E* **57**, 655 (1998).
- ¹⁶C. Bauer and S. Dietrich, *Eur. Phys. J. B* **10**, 767 (1999).
- ¹⁷A. I. Rusanov, *Colloids Surf., A* **156**, 315 (1999).
- ¹⁸A. Amirfazli and A. W. Neumann, *Adv. Colloid Interface Sci.* **110**, 121 (2004).
- ¹⁹L. Boruvka and A. W. Neumann, *J. Chem. Phys.* **66**, 5464 (1977).
- ²⁰S. Perković, I. Szeleifer, and B. Widom, *Mol. Phys.* **80**, 729 (1993).
- ²¹S. Perković, E. M. Blokhuis, E. Tessler, and B. Widom, *J. Chem. Phys.* **102**, 7584 (1995).
- ²²E. H. Hauge and M. Schick, *Phys. Rev. B* **27**, 4288 (1983).
- ²³J. O. Indekeu, *Physica A* **183**, 439 (1992).
- ²⁴C. Varea and A. Robledo, *Phys. Rev. E* **47**, 3772 (1993).
- ²⁵B. Widom and A. S. Clarke, *Physica A* **168**, 149 (1990).
- ²⁶B. Widom, in *Condensed Matter Theories*, edited by L. Blum and F. B. Malik (Plenum, New York, 1993), Vol. 8, pp. 589–593.
- ²⁷B. Widom, *J. Chem. Phys.* **68**, 3878 (1978).
- ²⁸B. Pluis, A.W. Denier van der Gon, and J. F. van der Veen, *Surf. Sci.*

239, 265 (1990).

²⁹R. Rosenberg, Phys. Today **58**, 50 (2005).

³⁰M. Elbaum, S. G. Lipson, and J. G. Dash, J. Cryst. Growth **129**, 491 (1993).

³¹C. M. Taylor and B. Widom, Physica A **358**, 492 (2005).

³²C. M. Taylor and B. Widom, Mol. Phys. **103**, 647 (2005).

³³K. Koga and B. Widom, Mol. Phys. **104**, 3469 (2006).

³⁴J. Kerins and M. Boiteux, Physica A **117**, 575 (1983).

³⁵W. H. Press, B. P. Flannery, S. A. Teukolsky, and W. T. Vetterling, *Numerical Recipes in C* (Cambridge University Press, Cambridge, 1998).